Arteriosclerosis, Thrombosis, and Vascular Biology

JOURNAL OF THE AMERICAN HEART ASSOCIATION

Long Pentraxin 3/Tumor Necrosis Factor-Stimulated Gene-6 Interaction : A Biological Rheostat for Fibroblast Growth Factor 2 –Mediated Angiogenesis

Daria Leali, Antonio Inforzato, Roberto Ronca, Roberta Bianchi, Mirella Belleri, Daniela Coltrini, Emanuela Di Salle, Marina Sironi, Giuseppe Danilo Norata, Barbara Bottazzi, Cecilia Garlanda, Anthony J. Day and Marco Presta

Arterioscler Thromb Vasc Biol 2012, 32:696-703: originally published online January 19, 2012
doi: 10.1161/ATVBAHA.111.243998
Arteriosclerosis, Thrombosis, and Vascular Biology is published by the American Heart Association. 7272 Greenville Avenue, Dallas, TX 72514
 Print ISSN: 1079-5642. Online ISSN: 1524-4636

Long Pentraxin 3/Tumor Necrosis Factor-Stimulated Gene-6 Interaction

A Biological Rheostat for Fibroblast Growth Factor 2–Mediated Angiogenesis

Daria Leali, Antonio Inforzato, Roberto Ronca, Roberta Bianchi, Mirella Belleri, Daniela Coltrini, Emanuela Di Salle, Marina Sironi, Giuseppe Danilo Norata, Barbara Bottazzi, Cecilia Garlanda, Anthony J. Day, Marco Presta

Objective—Angiogenesis is regulated by the balance between pro- and antiangiogenic factors and by extracellular matrix protein interactions. Fibroblast growth factor 2 (FGF2) is a major proangiogenic inducer inhibited by the interaction with the soluble pattern recognition receptor long pentraxin 3 (PTX3). PTX3 is locally coexpressed with its ligand tumor necrosis factor-stimulated gene-6 (TSG-6), a secreted glycoprotein that cooperates with PTX3 in extracellular matrix assembly. Here, we characterized the effect of TSG-6 on PTX3/FGF2 interaction and FGF2-mediated angiogenesis.

Methods and Results—Solid phase binding and surface plasmon resonance assays show that TSG-6 and FGF2 bind the PTX3 N-terminal domain with similar affinity. Accordingly, TSG-6 prevents FGF2/PTX3 interaction and suppresses the inhibition exerted by PTX3 on heparan sulfate proteoglycan/FGF2/FGF receptor complex formation and on FGF2-dependent angiogenesis in vitro and in vivo. Also, endogenous PTX3 exerts an inhibitory effect on vascularization induced by FGF2 in a murine subcutaneous Matrigel plug assay, the inhibition being abolished in *Ptx3*-null mice or by TSG-6 treatment in wild-type animals.

Conclusion—TSG-6 reverts the inhibitory effects exerted by PTX3 on FGF2-mediated angiogenesis through competition of FGF2/PTX3 interaction. This may provide a novel mechanism to control angiogenesis in those pathological settings characterized by the coexpression of TSG-6 and PTX3, in which the relative levels of these proteins may fine-tune the angiogenic activity of FGF2. **(*Arterioscler Thromb Vasc Biol*. 2012;32:696-703.)**

Key Words: angiogenesis ■ endothelium ■ FGF2 ■ TSG-6 ■ pentraxin

Angiogenesis, the process of new blood vessel formation from preexisting blood vessels, plays a key role in various physiological and pathological conditions, including wound healing, inflammation, and cancer.[1] The local, uncontrolled release of angiogenic growth factors and changes in the production of natural angiogenic inhibitors lead to disturbance of the angiogenic balance,[2] which is responsible for the uncontrolled neovascularization that takes place during tumor growth and angiogenesis-dependent diseases.[3]

Fibroblast growth factor 2 (FGF2) is a major heparin-binding angiogenic inducer.[4] Growing evidence suggests that there is a tight cross-talk between inflammatory and angiogenic responses during FGF2-mediated neovascularization (reviewed in[4]). Indeed, elevated levels of FGF2 have been implicated in the pathogenesis of several diseases characterized by a deregulated angiogenic/inflammatory response, including cancer.[4] FGF2 exerts its angiogenic activity by interacting with tyrosine-kinase FGF receptors (FGFRs)[5] and heparan sulfate proteoglycans (HSPGs) on the surface of endothelial cells (ECs) and within the extracellular matrix (ECM),[6,7] leading to the formation of productive HSPG/FGF2/FGFR ternary complexes that provide proangiogenic signals.[8] FGF2-dependent angiogenesis is further modulated by a complex network of interactions involving serum and ECM proteins and their degradation products.[9]

Received on: October 27, 2010; final version accepted on: January 4, 2012.

From the Unit of General Pathology and Immunology (D.L., R.R., R.B., M.B., E.D.S., M.P.) and Unit of Histology (D.C.), Department of Biomedical Sciences and Biotechnology, School of Medicine, University of Brescia, Brescia, Italy; Istituto di Ricovero e Cura a Carattere Scientifico Humanitas, Rozzano, Italy (A.I., M.S., B.B., C.G.); Department of Pharmacological Sciences, University of Milan, Milan, Italy (G.D.N.); Wellcome Trust Centre for Cell-Matrix Research, Faculty of Life Sciences, University of Manchester, Manchester, United Kingdom (A.I., A.J.D.).

Drs Leali and Inforzato contributed equally to this work.

The online-only Data Supplement is available with this article at http://atvb.ahajournals.org/lookup/suppl/doi:10.1161/ATVBAHA.111.243998/-/DC1.

Correspondence to Marco Presta, Department of Biomedical Sciences and Biotechnology, Viale Europa 11, 25123 Brescia, Italy (E-mail presta@med.unibs.it); or Anthony J. Day, Wellcome Trust Centre for Cell-Matrix Research, Faculty of Life Sciences, University of Manchester, Michael Smith Building, Oxford Road, Manchester M13 9PT, United Kingdom (E-mail anthony.day@manchester.ac.uk).

The soluble pattern recognition receptor pentraxin 3 (PTX3), also called tumor necrosis factor-stimulated gene (TSG)-14,[10] is the prototypic member of the long pentraxin family.[11] The mature PTX3 protein is composed of 8 identical subunits held together by a disulfide bond network, where each protomer is comprised of a C-terminal pentraxin domain (as found in the short pentraxins) and a unique N-terminal region.[12,13] PTX3 is an ECM-associated protein produced at sites of inflammation by monocytes, ECs and smooth muscle cells in response to inflammatory cytokines and bacterial components,[10,11,14,15] where all of these cell types are also major sources of FGF2 in vivo. PTX3 is believed to be an inflammatory mediator with unique and nonredundant functional roles at the crossroads of innate immunity (eg, mediating complement activation and providing protection against opportunistic pathogens), fertility, and angiogenesis.[11,16] This broad spectrum of biological activity is likely due to the structural complexity of the octameric PTX3 protein, shown recently to correspond to an elongated and asymmetric molecule composed of 2 differently sized globular lobes connected by a short stalk,[13] in which the N- and C-terminal regions of PTX3 mediate the binding to multiple ligands.[13,17,18] In this regard, PTX3 binds FGF2 with high affinity and specificity[19] via its N-terminal region.[13,20] Recent work indicates that each PTX3 octamer can bind to 2 FGF2 molecules where these binding sites are composed of tetrameric assemblies of the N-terminal domain.[13] Importantly, PTX3 inhibits FGF2-dependent EC proliferation in vitro and angiogenesis in vivo.[19,21,22] Also, PTX3 inhibits FGF2-dependent smooth muscle cell activation and intimal thickening after arterial injury.[23] Thus, PTX3 may contribute to the modulation of FGF2 activity in different pathological settings characterized by the coexpression of the 2 proteins, such as inflammation, atherosclerosis, and neoplasia (see[19,23] for further discussion).

TSG-6, the secreted product of tumor necrosis factor-stimulated gene-6 (also known as TNFAIP6), is an ≈35-kDa protein, composed mainly of a Link module[24] and a CUB_C domain,[25] that is expressed by a wide variety of cell types, including leukocytes, smooth muscle cells, and ECs in response to inflammatory stimuli.[26–30] For example, TSG-6 is expressed by vascular smooth muscle cells following blood vessel injury and mechanical strain[31,32] and has been detected at sites of neovascularization in the synovium of patients with rheumatoid arthritis.[33] TSG-6 has been implicated in ECM assembly and remodeling, where it binds to a wide range of ECM components,[29,30] including the glycosaminoglycan hyaluronan (HA),[24,34] the heavy chains of inter-α-inhibitor,[35,36] and PTX3.[37] Interestingly, TSG-6, HA, inter-α-inhibitor, and PTX3 all cooperate in the formation of an ECM around the preovulatory oocyte,[35,37,38] where the production of this matrix is required for successful ovulation and fertilization in vivo, and the interaction of TSG-6 with PTX3 may contribute directly to matrix stabilization via the formation of PTX3/TSG-6/HA complexes.[37] Notably, the coordinated expression of TSG-6 and PTX3 by leukocytes (in inflammatory infiltrates) and ECs has recently been described in inflamed tissues.[26] However, the effect of TSG-6 on the interaction of PTX3 with FGF2 and its antiangiogenic activity has not yet been investigated.

In this study, we demonstrate that TSG-6 reverts the inhibitory effects exerted by PTX3 on FGF2-mediated angiogenesis through competition of the FGF2/PTX3 interaction, pointing to a novel mechanism of modulation of the angiogenic process where the relative levels of TSG-6 and PTX3 dictate the biological activity of FGF2.

Methods

The detailed descriptions of the methods that were used in this study are provided in the online-only Data Supplement.

Solid Phase Binding Assays

Ninety-six-well microtiter plates were coated with PTX3, N-terminal (N_{term}) PTX3 or C-terminal (C_{term}) PTX3, TSG-6, Link_TSG6, or CUB_C_TSG6 and incubated with the proteins being tested for 1 hour at 37°C. Bound proteins were detected using the corresponding primary antibody. In competition experiments, bound biotinylated PTX3 (bPTX3) was revealed by incubation with alkaline phosphatase-conjugated streptavidin, and absorbance was read at 405 nm.

Surface Plasmon Resonance

A BIAcore X system (BIAcore Inc, Piscataway, NJ) was used to analyze the binding of FGF2, wild-type and TSG-6 mutants, Link_TSG6, and CUB_C_TSG6 to PTX3 immobilized on CM4 sensor chips.[20]

Cross-Linking Assay

FGF2 (11 pmol) was incubated for 1 hour at room temperature with PTX3 (55 pmol) in a 30-μL volume of phosphate-buffered saline (PBS) containing 1.25 mmol/L bis[sulfosuccinimidyl]suberate in the absence or presence of TSG-6 (110 pmol). Reaction products were separated by SDS-PAGE and revealed by Western blotting with either anti-FGF2 or anti-PTX3 antibodies.

FGF2-Mediated Cell-Cell Adhesion Assay

FGFR1-overexpressing, HSPG-deficient Chinese hamster ovary cells (A745 CHO flg-1A; 50 000 cells/cm^2) were incubated on glutaraldehyde-fixed wild-type CHO-K1 cell monolayers with or without 1.66 nmol/L of FGF2 in the absence or presence of PTX3 or N_{term}PTX3 (220 nmol/L) and increasing doses of TSG-6. After 2 hours at 37°C, A745 CHO flg-1A cells bound to the CHO-K1 cell monolayers were counted.[39]

EC Proliferation Assay

Subconfluent cultures of ECs were incubated in medium containing 0.4% (vol/vol) fetal calf serum plus FGF2 (0.55 nmol/L) in the absence or presence of PTX3 (220 nmol/L) and increasing doses of wild-type or TSG-6 mutants or Link_TSG6. Following 24 hours of incubation, cells were trypsinized and counted.[20]

Chicken Embryo Chorioallantoic Membrane Assay

Alginate beads containing vehicle or FGF2 (8 pmol) with or without PTX3 (33 pmol) and TSG-6 (83 pmol) were placed on top of the chorioallantoic membrane (CAM) at day 11 of incubation. After 72 hours, blood vessels converging toward the implant were counted under a stereomicroscope by 2 observers in a double-blind fashion.[40]

Matrigel Plug Angiogenesis Assay

Six-week-old female C57BL/6 wild-type and *Ptx3*$^{-/-}$[41] mice were injected subcutaneously with 400 μL of Matrigel containing PBS or 4.0 pmol of FGF2, 33 pmol of TSG-6, or both. After 7 days, pellets were processed for total RNA extraction, and the levels of expression of PTX3, FGF2, TSG-6, and vascular endothelial growth factor-A were assayed by semiquantitative reverse transcription–polymerase chain reaction in representative samples. The vascular response was quantified by evaluation of the levels of expression of the endothelial marker CD31 by quantitative reverse transcription–polymerase chain reaction.

Immunohistochemistry

Sections of human atherosclerotic carotid artery specimens, human gastric carcinoma, and human pleomorphic parotid adenoma biopsies were immunostained with anti-human PTX3, anti-human TSG-6, and anti-human FGF2 polyclonal antibodies.

Throughout this article, PTX3 concentrations are expressed as concentrations of PTX3 protomer.

Results

TSG-6 Binds the N-Terminal Domain of PTX3 via the Link Module

Previous observations suggest that TSG-6 interacts with PTX3 through its Link module at a distinct site from the HA-binding surface.[37] As shown in Figure 1A, PTX3 bound to microtiter plates coated with full-length human TSG-6 or with its Link module domain (Link_TSG6), whereas little or no interaction was observed when a recombinant preparation of the CUB_C domain (CUB_C_TSG6) was applied. Accordingly, real-time surface plasmon resonance analysis showed that both full-length TSG-6 and Link_TSG6, but not CUB_C_TSG6, bound PTX3 immobilized to the sensor chip (Figure 1B). Kinetic fitting of sensorgrams gave equilibrium dissociation constants (k_d) of 314 and 648 nmol/L for the binding of full-length TSG-6 and Link_TSG6 to PTX3, respectively (Figure I in the online-only Data Supplement). Similar results were obtained when Scatchard plot regression was performed on binding data acquired under steady-state conditions (data not shown).

Consistent with the observation that PTX3 and HA recognize distinct surfaces on TSG-6,[37] the TSG-$6_{Tyr94Phe}$ mutant, which has greatly reduced (≈100-fold) HA-binding activity ([42] and A.J. Day, unpublished data, 2010), has a similar affinity as wild-type TSG-6 for PTX3 (Figure I in the online-only Data Supplement). Conversely, the TSG-$6_{Tyr47Phe}$ mutant, which also has greatly impaired HA-binding activity (A.J. Day, unpublished data, 2010), binds PTX3 with somewhat lower affinity than wild-type TSG-6 (≈6-fold), suggesting that this amino acid may participate to some extent in PTX3 binding. Mutation of Glu183, located within the CUB module, to Ser (TSG-$6_{Glu183Ser}$) (A.J. Day, unpublished data, 2010), had no affect on PTX3 binding, consistent with the finding that the CUB_C domain did not play a part in the interaction (Figure I in the online-only Data Supplement). Taken together, these results demonstrate that the Link module, rather than the CUB_C domain, mediates the binding of TSG-6 to PTX3 and that this interaction occurs with an affinity similar to that reported for FGF2/PTX3 interaction (k_d=300 nmol/L[20]).

To identify which region of the PTX3 molecule is involved in the interaction with TSG-6, microtiter plates coated with recombinant forms of the N-terminal and C-terminal domains of PTX3 (N_{term}PTX3 and C_{term}PTX3, respectively) were incubated with TSG-6. As shown in Figure 2A, TSG-6 bound to immobilized N_{term}PTX3 in a concentration-dependent manner, similar to that seen with the full-length PTX3 protein, whereas no interaction of TSG-6 with C_{term}PTX3 was observed. Accordingly, Link_TSG6 bound immobilized full-length PTX3 and N_{term}PTX3 but not C_{term}PTX3, whereas CUB_C_TSG6 did not interact with any of the PTX3 domains (Figure 2B). Therefore, it can be concluded that PTX3 interacts with the Link module of TSG-6 via its N-terminal domain, which is also the site where FGF2 binds.[13,20,43]

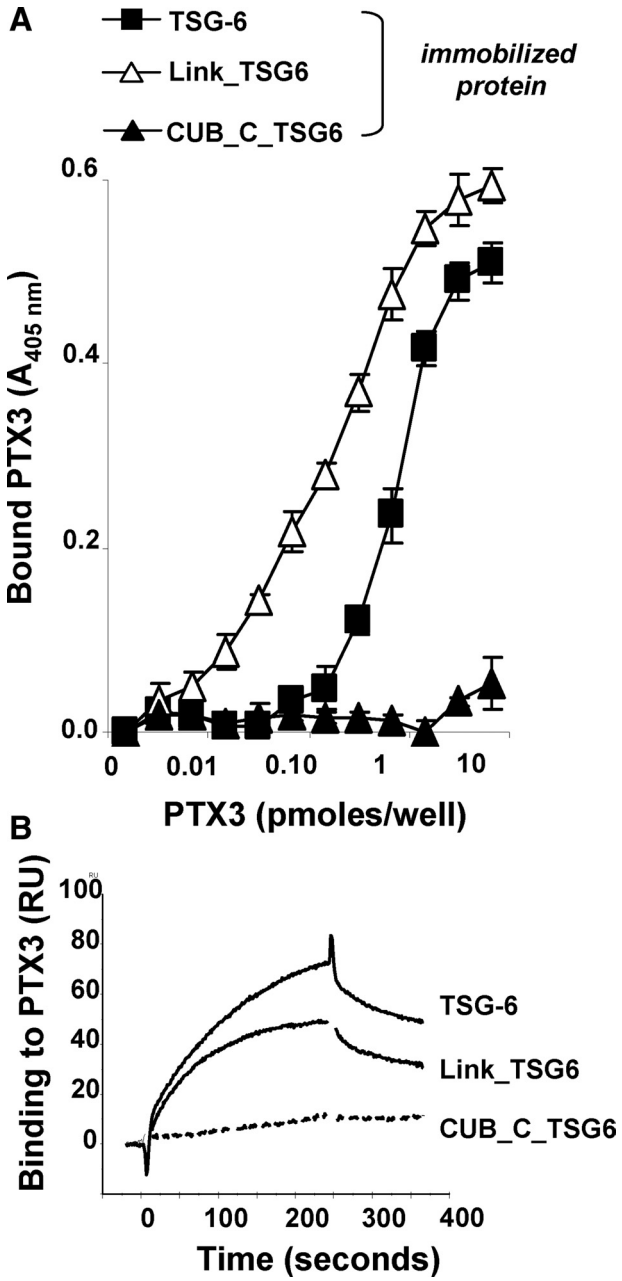

Figure 1. The Link module of TSG-6 binds pentraxin 3 (PTX3). **A**, Microtiter plates were coated with 25 pmol/well of TSG-6 (■), Link_TSG6 (△), or CUB_C_TSG6 (▲) and incubated with PTX3. Bound protein was detected using the anti-human PTX3 polyclonal antibody αPTX3pb. Data are expressed as mean±SD (n=12). **B**, TSG-6, Link_TSG6 and CUB_C_TSG6 were injected onto a PTX3-coated sensor chip, and protein binding was monitored by surface plasmon resonance (BIAcore). Sensorgrams are representative of the binding response at an analyte concentration of 300 nmol/L.

TSG-6 Inhibits the PTX3/FGF2 Interaction

As described above, TSG-6 and FGF2 both bind PTX3 with similar affinities where these interactions are mediated via the N-terminal region of PTX3. This suggests that TSG-6 might

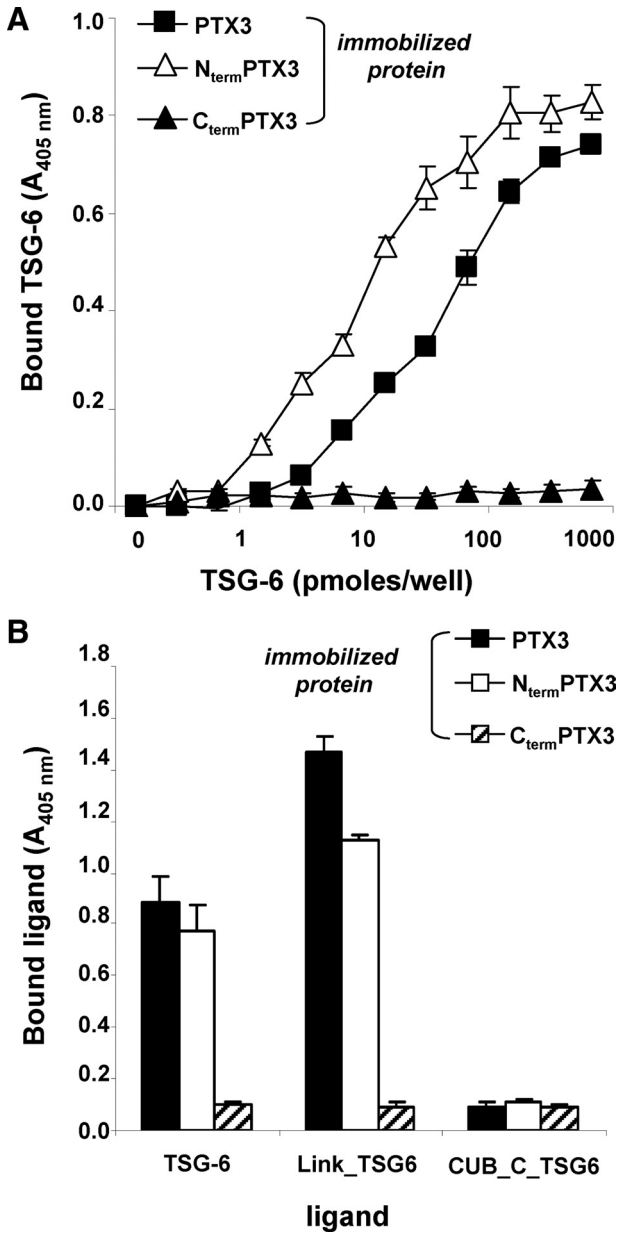

Figure 2. TSG-6 binds the N-terminal domain of pentraxin 3 (PTX3). **A**, Full-length PTX3 (■) or recombinant domains N-terminal (N_{term}) PTX3 (△) and C-terminal (C_{term}) PTX3 (▲) were immobilized on microtiter plates (15 pmol/well) and incubated with TSG-6. Bound TSG-6 was detected using the anti-human TSG-6 polyclonal antibody RAH1. **B**, Microtiter plates were coated with 15 pmol/well of full-length PTX3 (black bars), N_{term}PTX3 (white bars) or C_{term}PTX3 (hatched bars). Following incubation with full-length TSG-6, Link_TSG6, or CUB_C_TSG6 (all at 1 μmol/L), bound proteins were detected with RAH1 (for TSG-6 and CUB_C_TSG6) or Q75 (for Link_TSG6) antibodies. Data are expressed as mean±SD (n=12).

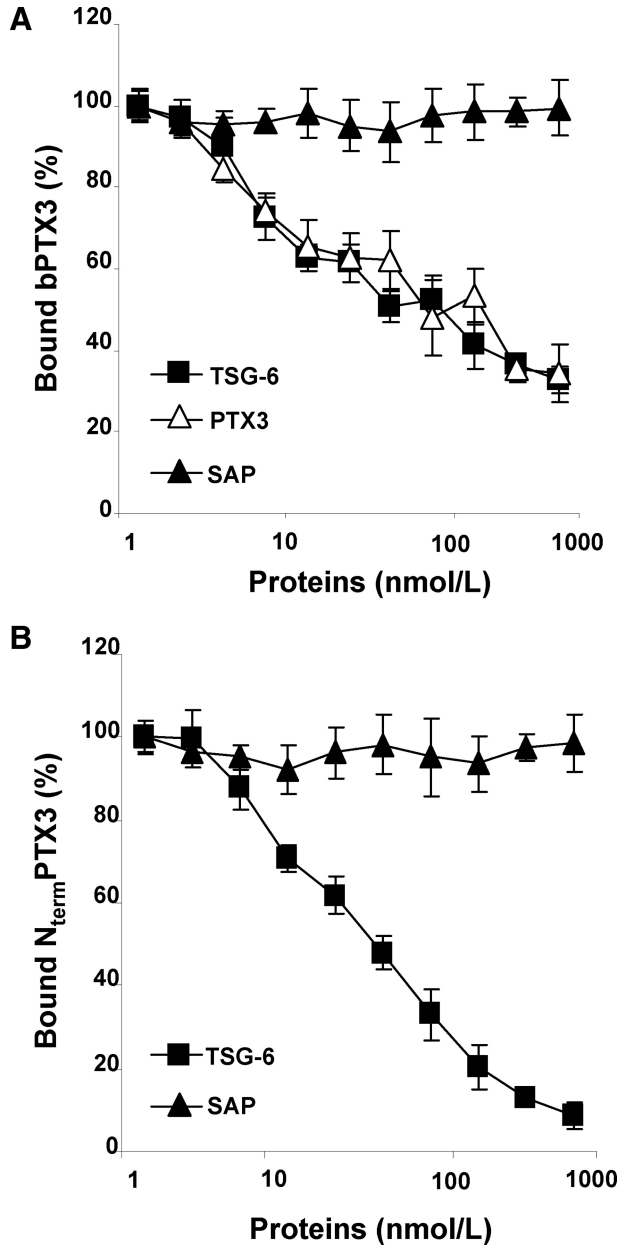

Figure 3. TSG-6 inhibits pentraxin 3 (PTX3)/fibroblast growth factor 2 (FGF2) interaction. **A**, Microtiter plates were coated with FGF2 (25 pmol/well) and incubated with 12 nmol/L biotinylated PTX3 (bPTX3) and various concentrations of TSG-6 (■). Bound bPTX3 was detected by incubation with ExtrAvidin, and absorbance was read at 405 nm. Nonbiotinylated PTX3 (△) and serum amyloid P component (SAP) (▲) were used as positive and negative controls, respectively. **B**, FGF2-coated microtiter plates were incubated with 50 nmol/L recombinant N-terminal (N_{term}) PTX3 and the indicated amounts of TSG-6 (■). Bound N_{term}PTX3 was detected with the αPTX3pb antibody. SAP was used as a negative control (▲). In both panels, data are the mean±SD of 3 independent experiments in quadruplicate and are expressed as percentage of ligand binding in the absence of competitors.

be able to modulate the interaction of PTX3 with FGF2. Indeed, TSG-6 competed for the binding of biotinylated PTX3 (bPTX3) to microtiter plates coated with FGF2 with a potency (IC_{50} ≈100 nmol/L) similar to that of nonbiotinylated PTX3, here used as a positive control (Figure 3A). Also, TSG-6 inhibits the binding of N_{term}PTX3 fragment to immobilized FGF2 (Figure 3B), whereas the short pentraxin serum amyloid P component, which is homologous to the C-terminal domain of PTX3 but does not bind FGF2 and TSG-6,[17] had no affect on bPTX3/FGF2 interaction. Furthermore, TSG-6 inhibited the chemical cross-linking of the FGF2/PTX3 complex in solution (Figure II in the online-only Data Supplement). Thus, TSG-6 acts as an inhibitor of the FGF2 interaction with PTX3.

TSG-6 Restores HSPG/FGF2/FGFR Ternary Complex Formation Inhibited by PTX3

FGF2 exerts its biological activity by leading to the formation of a proangiogenic HSPG/FGF2/FGFR ternary complex in ECs.[8] In keeping with its FGF2-antagonist activity, PTX3 inhibits the formation of this ternary complex in a cell-cell adhesion assay[39,44] in which FGF2 mediates the interaction of HSPG-deficient CHO cells stably transfected with FGFR1 to a monolayer of CHO cells expressing HSPGs but not FGFRs (Figure 4A). To investigate the effect of TSG-6 on the inhibitory activity exerted by PTX3 on HSPG/FGF2/FGFR ternary complex formation, cells were incubated with varying concentrations of TSG-6 in the presence of constant amounts of FGF2 and PTX3. As shown in Figure 4A, TSG-6 restored FGF2-mediated cell-cell adhesion (ie, the formation of the intercellular HSPG/FGF2/FGFR complex) in a dose-dependent fashion. It must be pointed out that TSG-6 alone (ie, in the absence of FGF2 and PTX3) did not induce cell-cell interaction, nor did it affect the FGF2-mediated formation of the HSPG/FGF2/FGFR complex when PTX3 was omitted. Similarly, TSG-6 also reversed the inhibitory effect of the N_{term}PTX3 fragment on HSPG/FGF2/FGFR complex formation (Figure III in the online-only Data Supplement). These data indicate that TSG-6 can rescue the PTX3-mediated inhibition of FGF2 engagement with its receptors, presumably via its competition for the PTX-FGF2 interaction.

TSG-6 Suppresses the Inhibitory Effect of PTX3 on FGF2-Dependent Angiogenesis

PTX3 inhibits the mitogenic activity exerted by FGF2 on ECs, without affecting the activity of unrelated mitogens.[19] On this basis, TSG-6 was assessed for its capacity to reverse the inhibition caused by PTX3 on FGF2-dependent EC proliferation. To this end, fetal bovine aortic GM7373 ECs were incubated with FGF2 (0.56 nmol/L), PTX3 (220 nmol/L), and a range of TSG-6 concentrations. Consistent with its ability to restore HSPG/FGF2/FGFR ternary complex formation inhibited by PTX3, increasing doses of TSG-6 progressively restored FGF2-induced EC proliferation in the presence of PTX3 (Figure 4B). A similar effect was also seen with the TSG-6 mutants TSG-$6_{Tyr47Phe}$, TSG-$6_{Tyr94Phe}$, and TSG-$6_{Glu183Ser}$ (Figure IV in the online-only Data Supplement), which all retain binding to PTX3 (see Figure I in the online-only Data Supplement). It should be noted that TSG-6 alone did not affect EC proliferation when tested in the absence or in the presence of FGF2 (Figure 4B).

To further confirm the capacity of TSG-6 to restore EC proliferation by preventing FGF2/PTX3 interaction, we took advantage of an experimental model in which human PTX3 or the N_{term}PTX3 fragment are endogenously expressed by retrovirus-infected murine aortic ECs (PTX3_MAECs and N_{term}PTX3_MAECs, respectively) and inhibit EC proliferation in response to exogenous FGF2.[20] As shown in Figure 4C and 4D, increasing doses of TSG-6 progressively restored the capacity of PTX3_MAEC and N_{term}PTX3_MAEC transfectants to proliferate in response to FGF2. Again, similar activities were seen with the TSG-6 mutant proteins (Figure IV in the online-only Data Supplement). These and the data

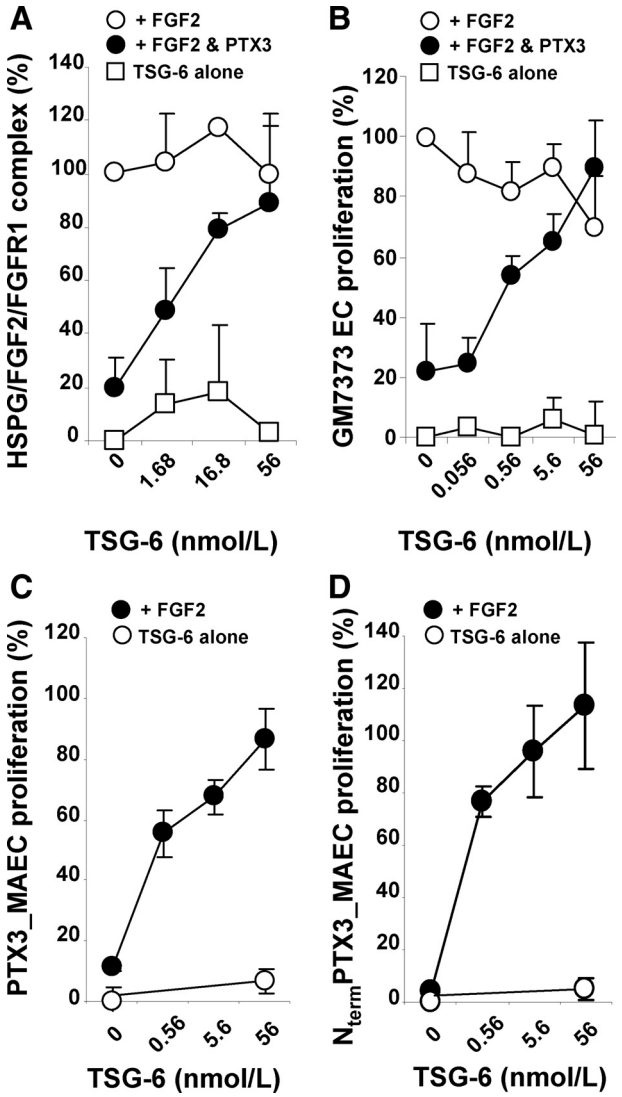

Figure 4. TSG-6 suppresses the inhibitory effect exerted by pentraxin 3 (PTX3) on fibroblast growth factor 2 (FGF2) activity. **A**, FGF receptor 1 (FGFR1)–overexpressing, heparan sulfate proteoglycan (HSPG)–deficient Chinese hamster ovary (CHO) cells were incubated on a monolayer of CHO-K1 cells with FGF2 (1.66 nmol/L) and the indicated amounts of TSG-6 in the absence (○) or presence (●) of PTX3 (220 nmol/L). After 2 hours, bound cells were counted under an inverted microscope. Data are expressed as percentage of the cell-cell adhesion induced by FGF2 alone. Binding of TSG-6-treated cells in the absence of FGF2 and PTX3 is shown as control (□). **B**, GM7373 cells were incubated with 0.4% fetal calf serum (FCS) containing 0.56 nmol/L FGF2 and the reported concentrations of TSG-6 in the absence (○) or presence (●) of PTX3 (220 nmol/L). After 24 hours, cells were trypsinized and counted. Data are expressed as percentage of GM7373 cells stimulated with FGF2 only. The proliferation of GM7373 cells treated with TSG-6 only (ie, in the absence of FGF2 and PTX3) is shown as a control (□). **C** and **D**, Retrovirus-infected PTX3 cells overexpressing PTX3 (PTX3_MAECs) (where MAEC indicates murine aortic EC) (**C**) or N-terminal (N_{term}) PTX3 (N_{term}PTX3_MAECs (**D**) were incubated with 0.4% FCS plus 0.56 nmol/L FGF2 and the indicated amounts of TSG-6 (●). Following 24 hours of incubation, cells were trypsinized and counted. Data are expressed as percentage of the proliferation measured in mock-infected cells stimulated with FGF2 only. The proliferation of cells treated with TSG-6 alone is shown as a control (○). In all graphs, intermediate markings on the *x* axis represent the actual concentrations of TSG-6 used in the different assays. Data are the mean±SD of 3 experiments performed in triplicate.

above demonstrate that neither the HA-binding function of TSG-6[24] nor its ability to form covalent complexes with the heavy chains of inter-α-inhibitor[36] (ie, properties impaired in these mutants) is necessary for TSG-6 to show activity in these angiogenesis assay systems.

The capacity of TSG-6 and PTX3 to affect FGF2-induced neovascularization in vivo was then investigated in a chicken embryo CAM angiogenesis assay[45] and in a murine subcutaneous Matrigel plug assay.[46] In the CAM assay, alginate beads adsorbed with FGF2 (8.0 pmol/embryo) exerted a potent angiogenic response when applied on the top of the CAM as compared with beads adsorbed with vehicle. Consistent with the in vitro observations, the angiogenic response elicited by FGF2 was significantly reduced by the addition of 33 pmol of PTX3 to the FGF2 implants ($P<0.001$), and this inhibition was fully abolished by coadministration of 83 pmol of TSG-6. No effect on CAM vascularization was instead exerted by TSG-6 alone (Figure 5A).

Next, the effect of TSG-6 on FGF2-induced angiogenesis was assessed in wild-type and *Ptx3*-null mice using a subcutaneous Matrigel plug assay (Figure 5B). It must be pointed out that the subcutaneous injection of Matrigel induces, per se, a mild proinflammatory reaction,[47] leading to the coexpression within the plug of PTX3, FGF2, TSG-6, and vascular endothelial growth factor-A transcripts (Figure V in the online-only Data Supplement). Also, no significant difference in the levels of FGF2, TSG-6, and vascular endothelial growth factor-A expression occurred in PBS-treated Matrigel plugs injected in *Ptx3*-null mice compared with plugs implanted in wild-type animals (Figure V in the online-only Data Supplement). Consistent with the FGF2-antagonist activity of PTX3, we observed a significant increase of vascularization in both PBS-treated and FGF2-treated plugs implanted in *Ptx3*-deficient mice compared with wild-type animals, as assessed by quantitative reverse transcription–polymerase chain reaction analysis of the levels of expression of the endothelial marker CD31 in the Matrigel plugs.[48] A similar increase was observed when TSG-6 was added to PBS-treated and FGF2-treated Matrigel plugs implanted in wild-type animals, no further significant increase in vascularization being exerted by TSG-6 in *Ptx3*-null mice (Figure 5B).

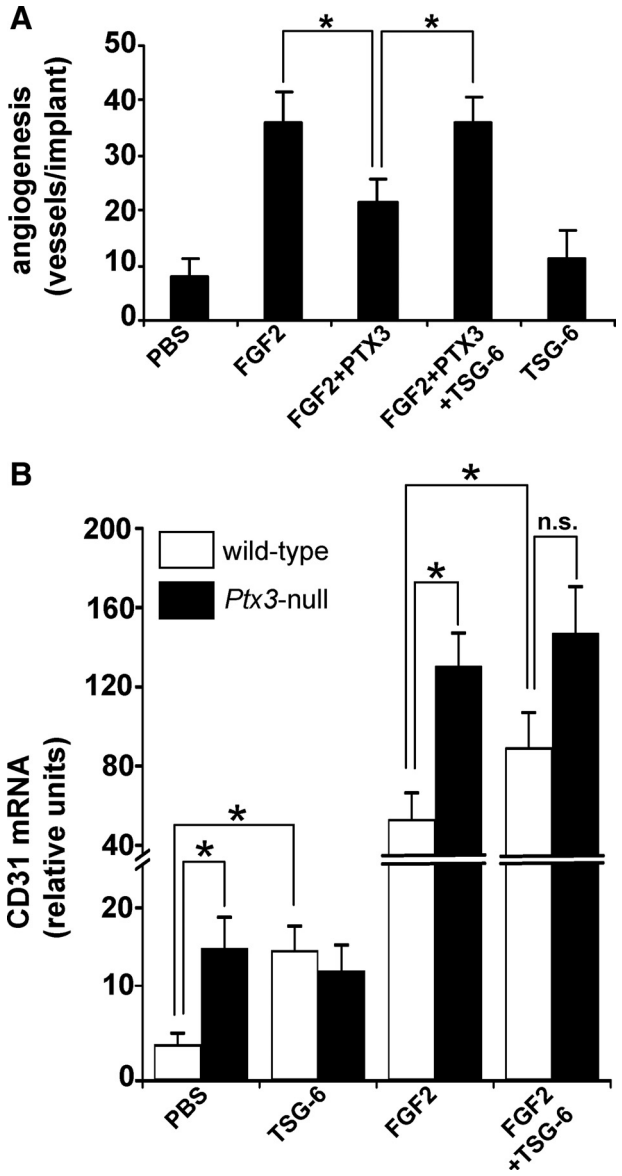

Figure 5. TSG-6/pentraxin 3 (PTX3) cross-talk modulates fibroblast growth factor 2 (FGF2)–mediated angiogenesis in vivo. **A**, Chicken embryo chorioallantoic membranes (CAMs) were implanted at day 11 with alginate beads containing FGF2 (8 pmol), PTX3 (33 pmol), and TSG-6 (83 pmol) or combinations of these proteins. At day 14, newly formed thin blood microvessels converging toward the implant in a spoke-wheel pattern (readily distinguishable from preexisting, larger vessels with no directionality)[45] were counted. CAM implants that contained vehicle (phosphate-buffered saline [PBS]) or TSG-6 only were used as controls. Data are the mean±SD (n=7–11). *$P<0.01$, Student *t* test. **B**, Wild-type (open bars) and *Ptx3*-null mice (black bars) were injected subcutaneously with Matrigel plugs containing PBS or 4 pmol of FGF2, 33 pmol of TSG-6, or both. After 7 days, pellets were processed for total RNA extraction, and the vascular response was quantified by reverse transcription–polymerase chain reaction analysis of the expression of the endothelial marker CD31. Data are the mean±SEM (n=8–10). *$P<0.05$ or better; n.s. indicates not statistically significant; Student *t* test.

Discussion

Taken together, the above results indicate that TSG-6 suppresses the inhibition exerted by PTX3 on FGF2-dependent angiogenesis both in vitro and in vivo. Thus, this provides the first direct evidence of a role for TSG-6 as a modulator of neovascularization. Our observations clearly indicate that TSG-6 exerts its "proangiogenic " functions via inhibition of the PTX3/FGF2 interaction, where this may be mediated by the binding of TSG-6 to PTX3. Preliminary solid phase binding and surface plasmon resonance assays suggest that TSG-6 may also interact directly with FGF2 (A. Inforzato and A.J. Day, unpublished data, 2009). Thus, TSG-6 might prevent FGF2/PTX3 interaction through a combination of mechanisms that together lead to suppression of the inhibition exerted by PTX3 on the angiogenic activity of FGF2. Further work is required to fully dissect the molecular interplay between PTX3, FGF2, and TSG-6 so as to understand the mechanism of TSG-6 action.

As described above, PTX3 may contribute to the modulation of FGF2-driven angiogenesis in different pathological settings characterized by the coexpression of the 2 proteins, including

inflammation, wound healing, atherosclerosis, and neoplasia (see[44,49] for further discussion). The coordinated expression of TSG-6 and PTX3 has been described in inflamed tissues[26,50] and in the cumulus oophorus.[37,50] Accordingly, FGF2, TSG-6, and PTX3 are coexpressed following subcutaneous injection of a Matrigel plug in mice (see Figure V in the online-only Data Supplement), a mildly proinflammatory experimental condition.[47] Moreover, immunohistochemical analysis performed on a limited series of human specimens shows that FGF2, TSG-6, and PTX3 are coexpressed in human atherosclerotic carotid artery and in biopsies of human benign tumors (pleomorphic parotid adenoma) and cancer (gastric carcinoma)[51,52] (Figure VI in the online-only Data Supplement). Additional studies on larger cohorts of patients will be required to assess the relationship between the expression of these modulators of the angiogenic process and tissue vascularization in different inflammatory/cancerous conditions.

Our study indicates that the relative levels of TSG-6 and PTX3 likely dictate the biological activity of FGF2; a low TSG-6:PTX3 ratio exerts an inhibitory effect on FGF2-mediated angiogenesis, whereas an high TSG-6:PTX3 ratio represents a permissive condition for the angiogenic activity of the growth factor. Thus, the interaction of TSG-6 and PTX3 might act as a biological rheostat for FGF2-dependent neovascularization, contributing to the complex extracellular protein interactome[9] that mediates the angiogenic process. These conclusions are supported by the observation that endogenous PTX3 exerts a significant inhibitory effect on vascularization induced by endogenous FGF2 or by the exogenously added growth factor in a murine Matrigel plug assay, this effect being abolished in *Ptx3*-null mice or by TSG-6 treatment in wild-type animals. As anticipated, no effect is exerted by TSG-6 in the absence of endogenous PTX3, ie, in *Ptx3*-null mice.

Our studies indicate that TSG-6 can act as a novel indirect proangiogenic cofactor by releasing FGF2 from the PTX3 constraints, no direct angiogenic activity being exerted by this protein when administered alone in the different assays. On the other hand, recent data have shown that intraocular TSG-6 treatment in a rat model of corneal wound healing can inhibit neovascularization,[53] possibly as a consequence of its anti-inflammatory activity (eg, inhibition of neutrophil infiltration).[30] Notably, the antiangiogenic and anti-inflammatory effects were observed only when TSG-6 was administered within 4 hours after injury, no effect being observed when the inflammatory cell infiltrate was already established.[30] Previous observations had shown that some anti-inflammatory cytokines, including erythropoietin[54] and interleukin-10[55] may promote angiogenesis, whereas tumor necrosis factor-α may exert pro- or antiangiogenic effects depending on the dose of the cytokine.[56] Taken together, these data suggest that TSG-6 may have both proangiogenic and antiangiogenic properties, such that the balance between promotion and inhibition of neovascularization may depend on context (eg, the microenvironment). Further research is needed to investigate the precise role of TSG-6 as a modulator of angiogenesis and how this is regulated, for example, by components of the ECM.

Acknowledgments

We thank Patrizia Dell'Era, Ragnar Lindstedt, and Giovanni Salvatori for reagents; Michela Corsini for having performed the CAM assays; and Manuela Nebuloni and Fabio Pasqualini for assistance with immunohistochemistry.

Sources of Funding

This work was supported by Arthritis Research UK (Grants 16539 and 18472), the Medical Research Council (Grant G0701180), and Sigma-Tau (to A.J.D.) and by Ministero dell'Istruzione, Università e Ricerca (Centro di Eccellenza per l'Innovazione Diagnostica e Terapeutica, Cofin Projects), Associazione Italiana per la Ricerca sul Cancro, and FIRB Project 2011 "Infiammazione e cancro" and Lombardy Innate Immunity Network Project (to M.P.). The contribution of the European Commission ("TOLERAGE" 2008-202156) and European Research Council (Project HIIS) (to A.I., M.S., B.B., and C.G.) is gratefully acknowledged. Dr Inforzato was the recipient of fellowships from Fondazione Italiana per la Ricerca sul Cancro, Fondazione "Humanitas" per la Ricerca, and Scuola Europea di Medicina Molecolare (SEMM).

Disclosures

None.

References

1. Carmeliet P, Jain RK. Angiogenesis in cancer and other diseases. *Nature*. 2000;407:249–257.
2. Hanahan D, Folkman J. Patterns and emerging mechanisms of the angiogenic switch during tumorigenesis. *Cell*. 1996;86:353–364.
3. Folkman J. Angiogenesis in cancer, vascular, rheumatoid and other disease. *Nat Med*. 1995;1:27–31.
4. Presta M, Dell'Era P, Mitola S, Moroni E, Ronca R, Rusnati M. Fibroblast growth factor/fibroblast growth factor receptor system in angiogenesis. *Cytokine Growth Factor Rev*. 2005;16:159–178.
5. Klint P, Claesson-Welsh L. Signal transduction by fibroblast growth factor receptors. *Front Biosci*. 1999;4:D165–D177.
6. Schlessinger J, Lax I, Lemmon M. Regulation of growth factor activation by proteoglycans: what is the role of the low affinity receptors? *Cell*. 1995;83:357–360.
7. Rusnati M, Presta M. Interaction of angiogenic basic fibroblast growth factor with endothelial cell heparan sulfate proteoglycans: biological implications in neovascularization. *Int J Clin Lab Res*. 1996;26:15–23.
8. Schlessinger J, Plotnikov AN, Ibrahimi OA, Eliseenkova AV, Yeh BK, Yayon A, Linhardt RJ, Mohammadi M. Crystal structure of a ternary FGF-FGFR-heparin complex reveals a dual role for heparin in FGFR binding and dimerization. *Mol Cell*. 2000;6:743–750.
9. Rusnati M, Presta M. Extracellular angiogenic growth factor interactions: an angiogenesis interactome survey. *Endothelium*. 2006;13:93–111.
10. Breviario F, d'Aniello EM, Golay J, Peri G, Bottazzi B, Bairoch A, Saccone S, Marzella R, Predazzi V, Rocchi M, et al. Interleukin-1-inducible genes in endothelial cells. Cloning of a new gene related to C-reactive protein and serum amyloid P component. *J Biol Chem*. 1992;267:22190–22197.
11. Mantovani A, Garlanda C, Bottazzi B. Pentraxin 3, a non-redundant soluble pattern recognition receptor involved in innate immunity. *Vaccine*. 2003;21(suppl 2):S43–S47.
12. Inforzato A, Rivieccio V, Morreale AP, Bastone A, Salustri A, Scarchilli L, Verdoliva A, Vincenti S, Gallo G, Chiapparino C, Pacello L, Nucera E, Serlupi-Crescenzi O, Day AJ, Bottazzi B, Mantovani A, De Santis R, Salvatori G. Structural characterization of PTX3 disulfide bond network and its multimeric status in cumulus matrix organization. *J Biol Chem*. 2008;283:10147–10161.
13. Inforzato A, Baldock C, Jowitt TA, Holmes DF, Lindstedt R, Marcellini M, Rivieccio V, Briggs DC, Kadler KE, Verdoliva A, Bottazzi B, Mantovani A, Salvatori G, Day AJ. The angiogenic inhibitor long pentraxin PTX3 forms an asymmetric octamer with two binding sites for FGF2. *J Biol Chem*. 2010;285:17681–17692.
14. Lee GW, Lee TH, Vilcek J. TSG-14, a tumor necrosis factor- and IL-1-inducible protein, is a novel member of the pentaxin family of acute phase proteins. *J Immunol*. 1993;150:1804–1812.
15. Vouret-Craviari V, Matteucci C, Peri G, Poli G, Introna M, Mantovani A. Expression of a long pentraxin, PTX3, by monocytes exposed to the mycobacterial cell wall component lipoarabinomannan. *Infect Immun*. 1997;65:1345–1350.
16. Deban L, Russo RC, Sironi M, Moalli F, Scanziani M, Zambelli V, Cuccovillo I, Bastone A, Gobbi M, Valentino S, Doni A, Garlanda C,

Danese S, Salvatori G, Sassano M, Evangelista V, Rossi B, Zenaro E, Constantin G, Laudanna C, Bottazzi B, Mantovani A. Regulation of leukocyte recruitment by the long pentraxin PTX3. *Nat Immunol*. 2010; 11:328–334.
17. Garlanda C, Bottazzi B, Bastone A, Mantovani A. Pentraxins at the crossroads between innate immunity, inflammation, matrix deposition, and female fertility. *Annu Rev Immunol*. 2005;23:337–366.
18. Presta M, Camozzi M, Salvatori G, Rusnati M. Role of the soluble pattern recognition receptor PTX3 in vascular biology. *J Cell Mol Med*. 2007; 11:723–738.
19. Rusnati M, Camozzi M, Moroni E, Bottazzi B, Peri G, Indraccolo S, Amadori A, Mantovani A, Presta M. Selective recognition of fibroblast growth factor-2 by the long pentraxin PTX3 inhibits angiogenesis. *Blood*. 2004;104:92–99.
20. Camozzi M, Rusnati M, Bugatti A, Bottazzi B, Mantovani A, Bastone A, Inforzato A, Vincenti S, Bracci L, Mastroianni D, Presta M. Identification of an antiangiogenic FGF2-binding site in the N terminus of the soluble pattern recognition receptor PTX3. *J Biol Chem*. 2006;281:22605–22613.
21. Nicoli S, Presta M. The zebrafish/tumor xenograft angiogenesis assay. *Nat Protoc*. 2007;2:2918–2923.
22. Nicoli S, De Sena G, Presta M. Fibroblast Growth Factor 2-induced angiogenesis in zebrafish: the zebrafish yolk membrane (ZFYM) angiogenesis assay. *J Cell Mol Med*. 2009;13:2061–2068.
23. Camozzi M, Zacchigna S, Rusnati M, Coltrini D, Ramirez-Correa G, Bottazzi B, Mantovani A, Giacca M, Presta M. Pentraxin 3 inhibits fibroblast growth factor 2-dependent activation of smooth muscle cells in vitro and neointima formation in vivo. *Arterioscler Thromb Vasc Biol*. 2005;25:1837–1842.
24. Kohda D, Morton CJ, Parkar AA, Hatanaka H, Inagaki FM, Campbell ID, Day AJ. Solution structure of the link module: a hyaluronan-binding domain involved in extracellular matrix stability and cell migration. *Cell*. 1996;86:767–775.
25. Kuznetsova SA, Mahoney DJ, Martin-Manso G, Ali T, Nentwich HA, Sipes JM, Zeng B, Vogel T, Day AJ, Roberts DD. TSG-6 binds via its CUB_C domain to the cell-binding domain of fibronectin and increases fibronectin matrix assembly. *Matrix Biol*. 2008;27:201–210.
26. Maina V, Cotena A, Doni A, Nebuloni M, Pasqualini F, Milner CM, Day AJ, Mantovani A, Garlanda C. Coregulation in human leukocytes of the long pentraxin PTX3 and TSG-6. *J Leukoc Biol*. 2009;86:123–132.
27. Wisniewski HG, Maier R, Lotz M, Lee S, Klampfer L, Lee TH, Vilcek J. TSG-6: a TNF-, IL-1-, and LPS-inducible secreted glycoprotein associated with arthritis. *J Immunol*. 1993;151:6593–6601.
28. Wisniewski HG, Vilcek J. TSG-6: an IL-1/TNF-inducible protein with anti-inflammatory activity. *Cytokine Growth Factor Rev*. 1997;8: 143–156.
29. Milner CM, Day AJ. TSG-6: a multifunctional protein associated with inflammation. *J Cell Sci*. 2003;116:1863–1873.
30. Milner CM, Higman VA, Day AJ. TSG-6: a pluripotent inflammatory mediator? *Biochem Soc Trans*. 2006;34:446–450.
31. Lee RT, Yamamoto C, Feng Y, Potter-Perigo S, Briggs WH, Landschulz KT, Turi TG, Thompson JF, Libby P, Wight TN. Mechanical strain induces specific changes in the synthesis and organization of proteoglycans by vascular smooth muscle cells. *J Biol Chem*. 2001;276: 13847–13851.
32. Ye L, Mora R, Akhayani N, Haudenschild CC, Liau G. Growth factor and cytokine-regulated hyaluronan-binding protein TSG-6 is localized to the injury-induced rat neointima and confers enhanced growth in vascular smooth muscle cells. *Circ Res*. 1997;81:289–296.
33. Bayliss MT, Howat SL, Dudhia J, Murphy JM, Barry FP, Edwards JC, Day AJ. Up-regulation and differential expression of the hyaluronan-binding protein TSG-6 in cartilage and synovium in rheumatoid arthritis and osteoarthritis. *Osteoarthritis Cartilage*. 2001;9:42–48.
34. Baranova NS, Nileback E, Haller FM, Briggs DC, Svedhem S, Day AJ, Richter RP. The inflammation-associated protein TSG-6 cross-links hyaluronan via hyaluronan-induced TSG-6 oligomers *J Biol Chem*. 2011; 286:25675–25686.
35. Fulop C, Szanto S, Mukhopadhyay D, Bardos T, Kamath RV, Rugg MS, Day AJ, Salustri A, Hascall VC, Glant TT, Mikecz K. Impaired cumulus mucification and female sterility in tumor necrosis factor-induced protein-6 deficient mice. *Development*. 2003;130:2253–2261.
36. Rugg MS, Willis AC, Mukhopadhyay D, Hascall VC, Fries E, Fulop C, Milner CM, Day AJ. Characterization of complexes formed between TSG-6 and inter-α-inhibitor that act as intermediates in the covalent transfer of heavy chains onto hyaluronan. *J Biol Chem*. 2005;280: 25674–25686.
37. Salustri A, Garlanda C, Hirsch E, De Acetis M, Maccagno A, Bottazzi B, Doni A, Bastone A, Mantovani G, Beck Peccoz P, Salvatori G, Mahoney DJ, Day AJ, Siracusa G, Romani L, Mantovani A. PTX3 plays a key role in the organization of the cumulus oophorus extracellular matrix and in in vivo fertilization. *Development*. 2004;131:1577–1586.
38. Scarchilli L, Camaioni A, Bottazzi B, Negri V, Doni A, Deban L, Bastone A, Salvatori G, Mantovani A, Siracusa G, Salustri A. PTX3 interacts with inter-α-trypsin inhibitor: implications for hyaluronan organization and cumulus oophorus expansion. *J Biol Chem*. 2007;282:30161–30170.
39. Leali D, Belleri M, Urbinati C, Coltrini D, Oreste P, Zoppetti G, Ribatti D, Rusnati M, Presta M. Fibroblast growth factor-2 antagonist activity and angiostatic capacity of sulfated Escherichia coli K5 polysaccharide derivatives. *J Biol Chem*. 2001;276:37900–37908.
40. Mitola S, Moroni E, Ravelli C, Andres G, Belleri M, Presta M. Angiopoietin-1 mediates the proangiogenic activity of the bone morphogenic protein antagonist Drm. *Blood*. 2008;112:1154–1157.
41. Garlanda C, Hirsch E, Bozza S, Salustri A, De Acetis M, Nota R, Maccagno A, Riva F, Bottazzi B, Peri G, Doni A, Vago L, Botto M, De Santis R, Carminati P, Siracusa G, Altruda F, Vecchi A, Romani L, Mantovani A. Non-redundant role of the long pentraxin PTX3 in antifungal innate immune response. *Nature*. 2002;420:182–186.
42. Selbi W, Day AJ, Rugg MS, Fulop C, de la Motte CA, Bowen T, Hascall VC, Phillips AO. Overexpression of hyaluronan synthase 2 alters hyaluronan distribution and function in proximal tubular epithelial cells. *J Am Soc Nephrol*. 2006;17:1553–1567.
43. Leali D, Bianchi R, Bugatti A, Nicoli S, Mitola S, Ragona L, Tomaselli S, Gallo G, Catello S, Rivieccio V, Zetta L, Presta M. Fibroblast growth factor 2-antagonist activity of a long-pentraxin 3-derived antiangiogenic pentapeptide. *J Cell Mol Med*. 2010;14:2109–2121.
44. Leali D, Alessi P, Coltrini D, Rusnati M, Zetta L, Presta M. Fibroblast growth factor-2 antagonist and antiangiogenic activity of long-pentraxin 3-derived synthetic peptides. *Curr Pharm Des*. 2009;15:3577–3589.
45. Ribatti D, Nico B, Vacca A, Presta M. The gelatin sponge-chorioallantoic membrane assay. *Nat Protoc*. 2006;1:85–91.
46. Akhtar N, Dickerson EB, Auerbach R. The sponge/Matrigel angiogenesis assay. *Angiogenesis*. 2002;5:75–80.
47. Andres G, Leali D, Mitola S, Coltrini D, Camozzi M, Corsini M, Belleri M, Hirsch E, Schwendener RA, Christofori G, Alcami A, Presta M. A pro-inflammatory signature mediates FGF2-induced angiogenesis. *J Cell Mol Med*. 2009;13:2083–2108.
48. Leali D, Alessi P, Coltrini D, Ronca R, Corsini M, Nardo G, Indraccolo S, Presta M. Long pentraxin-3 inhibits FGF8b-dependent angiogenesis and growth of steroid hormone-regulated tumors. *Mol Cancer Ther*. 2011;10:1600–1610.
49. Alessi P, Leali D, Camozzi M, Cantelmo A, Albini A, Presta M. Anti-FGF2 approaches as a strategy to compensate resistance to anti-VEGF therapy: long-pentraxin 3 as a novel antiangiogenic FGF2-antagonist. *Eur Cytokine Netw*. 2009;20:225–234.
50. Day AJ, de la Motte CA. Hyaluronan cross-linking: a protective mechanism in inflammation? *Trends Immunol*. 2005;26:637–643.
51. Miguita L, Martinez EF, de Araujo NS, de Araujo VC. FGF-2, TGFβ-1, PDGF-A and respective receptors expression in pleomorphic adenoma myoepithelial cells: an in vivo and in vitro study. *J Appl Oral Sci*. 2010;18:83–91.
52. Zhang W, Chu YQ, Ye ZY, Zhao ZS, Tao HQ. Expression of hepatocyte growth factor and basic fibroblast growth factor as prognostic indicators in gastric cancer. *Anat Rec (Hoboken)*. 2009;292:1114–1121.
53. Oh JY, Roddy GW, Choi H, Lee RH, Ylostalo JH, Rosa RH Jr, Prockop DJ. Anti-inflammatory protein TSG-6 reduces inflammatory damage to the cornea following chemical and mechanical injury. *Proc Natl Acad Sci U S A*. 2010;107:16875–16880.
54. Ribatti D, Presta M, Vacca A, Ria R, Giuliani R, Dell'Era P, Nico B, Roncali L, Dammacco F. Human erythropoietin induces a pro-angiogenic phenotype in cultured endothelial cells and stimulates neovascularization in vivo. *Blood*. 1999;93:2627–2636.
55. Hatanaka H, Abe Y, Naruke M, Tokunaga T, Oshika Y, Kawakami T, Osada H, Nagata J, Kamochi J, Tsuchida T, Kijima H, Yamazaki H, Inoue H, Ueyama Y, Nakamura M. Significant correlation between interleukin 10 expression and vascularization through angiopoietin/TIE2 networks in non-small cell lung cancer. *Clin Cancer Res*. 2001;7:1287–1292.
56. Heba G, Krzeminski T, Porc M, Grzyb J, Ratajska A, Dembinska-Kiec A. The time course of tumor necrosis factor-α, inducible nitric oxide synthase and vascular endothelial growth factor expression in an experimental model of chronic myocardial infarction in rats. *J Vasc Res*. 2001;38:288–300.

SUPPLEMENTAL MATERIAL

Leali et al. TSG-6 modulates angiogenesis

Detailed Methods

Purified proteins and chemicals

Recombinant human FGF2 and PTX3 expressed in *E. coli* and HEK-293F cell lines, respectively [1, 2], were provided by Tecnogen (Piana di Monteverna, Caserta, Italy). Biotinylated recombinant human PTX3 (bPTX3) and purified recombinant construct N_{term}PTX3 (spanning the N-terminal region of the human PTX3 protein; residues 18-170 of the preprotein [3]), were supplied by Dr. G. Salvatori (Sigma-Tau S.p.A.; Pomezia, Italy). The purified recombinant construct C_{term}PTX3, corresponding to the C-terminal pentraxin domain of the human PTX3 protein (residues 178-381 of the preprotein), was obtained from Dr. B. Bottazzi (Humanitas Clinical Institute, Rozzano, Italy). Recombinant full-length human TSG-6 (Q allele) and the TSG-6_{Y47F}, TSG-6_{Y94F} and TSG-6_{E183S} mutants were produced in *Drosophila* S2 cells as described ([4, 5] and A.J Day, unpublished data, 2010). The Link module from human TSG-6 (Link_TSG6; residues 36-133 of the preprotein [6]) was expressed in *E. coli* and purified as before [7, 8]. The CUB_C domain of human TSG-6 (CUB_C_TSG6; residues 129–277 of the Q allele preprotein) was expressed in *E. coli* as previously described [9]. Purified human serum amyloid P component (SAP) was from Calbiochem (La Jolla, CA).

Antibodies

Biotin-labeled rabbit anti-human PTX3 polyclonal antibody (αPTX3pb) and rat anti-human PTX3 monoclonal antibody (16B5) were obtained from Dr. B. Bottazzi. Rabbit anti-human FGF2 polyclonal antibody was purchased from MBL (Woburn, MA). Rabbit anti-human TSG-6 anti-serum (RAH1), which recognizes the last 16 amino acids of the human TSG-6 protein (residues 262-277), and supernatant from rat anti-human TSG-6 hybridoma (Q75), that recognizes the Link module of TSG-6, were produced as described in [10, 11], respectively. The rabbit anti-human FGF2 polyclonal antibody was kindly provided by Dr. P. Dell'Era, University of Brescia, Italy. Alkaline phosphatase (AP)-conjugated streptavidin (ExtrAvidin™), AP-conjugated goat anti-rat and anti-rabbit IgG antibodies were from Sigma Aldrich (St. Louis, MO).

Solid phase binding assays

Binding studies were carried out using either maxisorp or polysorp 96 well microtitre plates (Nunc,

Roskilde, Denmark). All dilutions, incubations, and washes were performed in 50 mmol/L HEPES, 100 mmol/L NaCl, 0.1% (v/v) Tween 20, pH 7.40 (HBS-T). Plates were coated overnight at room temperature with proteins in either 20 mmol/L Na_2CO_3, pH 9.6 (for maxisorp plates) or 10 mmol/L sodium phosphate, 140 mmol/L NaCl, 2.7 mmol/L KCl, pH 7.40 (for polysorp plates). Control wells were incubated with buffer alone and treated as for sample wells. Plates were blocked with 1% (w/v) bovine serum albumin (BSA) for 2 hours at 37 °C, and incubated with proteins for 1 hour at 37 °C. Bound proteins were detected using the appropriate primary antibody (αPTX3pb, RAH1, Q75 or anti-human FGF2 polyclonal antibody at 1:5,000, 1:8,000, 1:100 or 1:2,000 dilutions in HBS-T, respectively), followed by serial incubation with ExtrAvidin™ (1:5,000 dilution in HBS-T) or secondary antibody (AP-conjugated goat anti-rat or goat anti-rabbit IgGs at 1:2,000 or 1:5,000 dilutions in HBS-T) and the substrate disodium *p*-nitrophenyl phosphate (1 mg/mL) in 100 mmol/L Tris-HCl, 100 mmol/L NaCl, 5 mmol/L $MgCl_2$, pH 9.3. Absorbance was read at 405 nm and background from uncoated wells subtracted.

Inhibition experiments were also performed where FGF2-coated plates were incubated with solutions of biotinylated PTX3 (bPTX3) or N_{term}PTX3 in the presence of full-length TSG-6. Competition with non-biotinylated PTX3 and SAP were used as positive and negative controls, respectively. Bound bPTX3 was revealed by incubation with alkaline phosphatase-conjugated streptavidin (ExtrAvidin™, Sigma Aldrich) and absorbance was read at 405 nm. Data are expressed as percent inhibition of free bPTX3 binding.

Surface plasmon resonance assays

A BIAcore X apparatus (BIAcore Inc., Piscataway, NJ) was used to analyze the binding of wt/mutant TSG-6, Link_TSG6 and CUB_C_TSG6 to immobilized PTX3. 35 µL of PTX3 (2.2 µmol/L in 10 mmol/L sodium acetate, pH 2.4) was injected into the flow cell of a CM4 chip previously activated with a mixture of 0.2 mol/L N-ethyl-N'-(3-dimethylaminopropyl)-carbodiimide hydrochloride (EDC) and 0.05 mol/L N-hydroxysuccinimide (NHS) at a flow rate of 10 µL/minute. Following neutralization of free active carboxymethyldextran (35 µL of 1.0 mol/L ethanolamine, pH 8.5 at 10 µL/minute), approximately 0.1 pmoles PTX3/mm^2 were immobilized. A similar amount of gelatine was coupled to a different flow cell, which was used as a negative control and for blank subtraction. The analytes were injected over the ligand surface at concentrations ranging from 10 to 500 nmol/L in 0.01 mol/L HEPES, pH 7.4 containing 0.005% (v/v) surfactant P20, 0.15 mol/L NaCl, 3 mmol/L EDTA (HBS-EP) and the surface was regenerated by injection of 10 mmol/L NaOH (10 µL). Kinetic analyses were performed at a flow rate of 10 µL/minute and allowing a total association time of 4 minutes.

In all experiments, association and dissociation constants (k_{on} and k_{off}, respectively) were obtained by fitting the raw sensorgrams with the 1:1 Langmuir binding model using the Biaevaluation software (BIAcore). Equilibrium affinity constants (i.e. expressed as dissociation constant, k_d) were either derived from the kinetic parameters ($k_d = k_{off}/k_{on}$) or determined from Scatchard plots obtained under state steady conditions.

Chemical cross-linking

Cross-linking experiments were performed with Bis[sulfosuccinimidyl]suberate (BS^3) obtained from Pierce (Rockford, IL). FGF2 (11 pmoles) was incubated with PTX3 (55 pmoles) in 30 μL of PBS containing BS^3 (1.25 mmol/L) in the absence or presence of TSG-6 (110 pmoles, i.e. 10-fold molar excess of TSG-6 over FGF2) for 1 hour at room temperature. The reaction was terminated by addition of sample loading buffer and samples were boiled for 5 minutes at 95 °C. Reaction products were separated on Tris-glycine 6% (w/v) SDS-PAGE gels under reducing conditions and revealed by Western blotting using a purified rabbit anti-human FGF2 polyclonal antibody (1:200 dilution) followed by incubation with horse radish peroxidase (HRP)-conjugated goat anti-rabbit IgG antibody (1:5,000 dilution; Santa Cruz Biotechnology, Santa Cruz, CA). Alternatively, membranes were incubated with the rat anti-human PTX3 monoclonal antibody 16B5 (1:1,000 dilution) followed by HRP-conjugated rabbit anti-rat IgG antibody (1:5,000 dilution; Sigma).

Cell cultures

Fetal bovine aortic GM7373 endothelial cells [12] were grown in Dulbecco's modified Eagle's medium containing 10% (v/v) fetal calf serum (FCS). Wild-type CHO-K1 cells and the derived HSPG-deficient A745 CHO cell mutants [13], kindly provided by Dr. J. D. Esko (La Jolla, CA), were grown in Ham's F-12 medium supplemented with 10% FCS. FGFR1-transfected A745 CHO flg-1A cells, bearing about 30,000 FGFR1 molecules/cell, were generated by transfection with the IIIc variant of murine FGFR1 cDNA [14]. Balb/c murine aortic 22106 ECs (MAECs) were obtained from Dr. R. Auerbach (University of Wisconsin, Madison, WI) and grown in Dulbecco's modified Eagle's medium supplemented with 10% FCS. MAECs overexpressing the enhanced green fluorescent protein (EGFP-MAECs), the N-terminal fragment PTX3-(1–178) (N_{term}PTX3-MAECs) or full length PTX3 (PTX3-MAECs) were generated by infection with retrovirus harbouring the corresponding cDNAs as described previously [15].

FGF2-mediated cell-cell adhesion assay

This assay was performed as described previously [16], with minor modifications. Briefly, wild-type CHO-K1 cells were seeded in 24-well plates at 150,000 cells/cm^2. After 24 hours, cell monolayers were washed with PBS and incubated with 3% (v/v) glutaraldehyde in PBS for 2 hours at 4 °C. Fixation was stopped with 0.1 mol/L glycine and cells were washed extensively with PBS. Then, A745 CHO flg-1A cells (50,000 cells/cm^2) were added to CHO-K1 monolayers in serum-free medium *plus* 10 mmol/L EDTA with or without 1.66 nmol/L FGF2 in the absence or presence of PTX3 or N_{term}PTX3 (both at 220 nmol/L) and increasing doses of TSG-6. After 2 hours of incubation at 37 °C, unattached cells were removed by washing twice with PBS, and A745 CHO flg-1A cells bound to the CHO-K1 monolayer were counted under an inverted microscope at ×125 magnification. Adherent A745 CHO flg-1A cells have a rounded morphology and can be easily distinguished from the confluent CHO-K1 monolayer lying underneath on a different plane of focus. Data are expressed as the mean of the cell counts of three microscopic fields chosen at random. All experiments were performed in duplicate and repeated twice with similar results.

Cell proliferation assays

GM7373 cell and MAEC proliferation assays were performed as described [15] with minor modifications. Briefly, subconfluent cultures of GM7373 cells or MAECs were incubated in medium containing 0.4% FCS *plus* FGF2 (0.55 nmol/L) in the absence or in the presence of PTX3 (220 nmol/L) and increasing doses of TSG-6, TSG-6 mutants or Link_TSG6. For all the assays, cells were trypsinized and counted in a Burker chamber after 24 hours of incubation.

Chick embryo chorioallantoic membrane assay

Alginate beads (4 μL) containing vehicle or 8 pmoles of FGF2 with or without PTX3 (33 pmoles) and TSG-6 (83 pmoles) were prepared as described [17, 18] and placed on top of the chicken embryo chorioallantoic membrane (CAM) of fertilized White Leghorn chicken eggs at day 11 of incubation (10 eggs per experimental group). After 72 hours, newly-formed thin blood microvessels converging toward the implant in a spoke-wheel pattern (easily distinguishable from preexisting, larger vessels with no directionality)[17] were counted by two observers in a double-blind fashion under a stereomicroscope (STEMI-SR, x2/0.12; Zeiss).

Matrigel plug angiogenesis assay

Six week old female C57BL/6 wild type and *Ptx3*-null [19] mice were injected s.c. with 400 μL of Matrigel (Trevigen, Gaithersburg, MD) containing PBS or 4 pmoles of FGF2 and/or 33 pmoles of

TSG-6. After 7 days, pellets were processed for total RNA extraction and the vascular response was quantified by RT-PCR analysis of the expression of the endothelial marker CD31 [20]. To this purpose, total RNA was extracted from Matrigel plugs using TRIzol Reagent according to manufacturer's instructions (Invitrogen, Carlsbad, CA). Purified total RNA was dissolved in RNase free water at 1:1 (w:v) ratio and contaminating DNA was digested using DNase, following the protocol reported in DNase 1 Amplification Grade kit (Sigma-Aldrich, Saint Louis, MO). Four μL of total RNA were retrotranscribed with MMLV reverse transcriptase (Invitrogen, Carlsbad, CA) using random hexaprimers in a final 20 μL volume. Quantitative PCR was performed with a Biorad iCycler iQ™ Real-Time PCR Detection System using a iQ™ SYBR Green Supermix (Biorad) according to manufacturer's instructions. Each PCR reaction was performed in triplicate on one plate and fluorescence data were recorded using iCycler software (BioRad). Also, the levels of endogenous PTX3, FGF2, TSG-6 and VEGF-A expression were assayed by semi-quantitative RT-PCR in representative samples.

The following primers were used:

murine CD31, 5'-CGGTTATGATGATGTTTCTGGA (forward) and
5'-AAGGGAGGACACTTCCACTTCT (reverse);

murine PTX3, 5'-GACCTCGGATGACTACGAG (forward) and
5'-CTCCGAGTGCTCCTGGCG(reverse);

murine FGF2, 5'-TCAAACTACAACTCCAAGCAGAA (forward) and
5'-GTAACACACTTAGAAGCCAGCA (reverse);

murine TSG-6, 5'- GGCTCACGGATGGGGATTCA (forward) and
5'- GGTTGCGAGACGACCACCTTCA (reverse);

murine VEGF-A, 5'-ACCTCCACCATGCCAAGT (forward) and
5'- TCAATCGGACGGCAGTAG (reverse);

murine GAPDH, 5'-GAAGGTCGGTGTGAACGGATT (forward) and
5'-TGACTGTGCCGTTGAATTTG (reverse).

Immunohistochemistry

Frozen specimens of human atherosclerotic carotid artery were fixed for 15 minutes with 4% (v/v) paraformaldehyde (PFA). Gastric carcinoma and pleomorphic parotid adenoma biopsies were formalin-fixed and paraffin-embedded. Three μm sections of each sample were mounted onto Super-frost slides (Bio-Optica, Milan, Italy), dewaxed with xylene and rehydrated with ethanol. Antigen retrieval was performed at 800W in 0.25 mmol/L EDTA (2 cycles of 3 minutes each). Endogenous peroxidase of both frozen and formalin-fixed tissues was blocked with PeroxAbolish

and Peroxidazed 1 (BioCare Medical, San Francisco, CA) and unspecific sites were blocked with Background Sniper (BioCare Medical) or 2% FCS in PBS for PTX3 and FGF2 and for TSG-6, respectively). Sections were incubated with either rabbit anti-human PTX3 (250 ng/mL), rabbit anti-human TSG-6 (RAH-1; 1:1000 dilution) or goat anti-human FGF2 (R&D Systems, Minneapolis, MN; 1:200 dilution) polyclonal antibodies (2 hours at room temperature for PTX3; overnight at 4°C for TSG-6 and FGF2) followed by Envision anti Rabbit HRP (Dako, Glostrup, Denmark; for PTX3 and TSG-6) and goat HRP polymer (BioCare Medical; for FGF2). Staining reactions were revealed with 3,3′-diaminobenzidine (DAB) free base as chromogen (brown staining, BioCare Medical).

Supplemental References

1. Isacchi A, Statuto M, Chiesa R, Bergonzoni L, Rusnati M, Sarmientos P, Ragnotti G, Presta M. A six-amino acid deletion in basic fibroblast growth factor dissociates its mitogenic activity from its plasminogen activator-inducing capacity. *Proc Natl Acad Sci U S A.* 1991;88:2628-2632.
2. Rivieccio V, Esposito A, Bellofiore P, Palladino P, Sassano M, Colombo M, Verdoliva A. High-level expression and efficient purification of recombinant human long pentraxin PTX3 in Chinese hamster ovary cells. *Protein Expr Purif.* 2007;51:49-58.
3. Breviario F, d'Aniello EM, Golay J, Peri G, Bottazzi B, Bairoch A, Saccone S, Marzella R, Predazzi V, Rocchi M, Della Valle G, Dejana E, Mantovani A, Introna M. Interleukin-1-inducible genes in endothelial cells. Cloning of a new gene related to C-reactive protein and serum amyloid P component. *J Biol Chem.* 1992;267:22190-22197.
4. Nentwich HA, Mustafa Z, Rugg MS, Marsden BD, Cordell MR, Mahoney DJ, Jenkins SC, Dowling B, Fries E, Milner CM, Loughlin J, Day AJ. A novel allelic variant of the human TSG-6 gene encoding an amino acid difference in the CUB module. Chromosomal localization, frequency analysis, modeling, and expression. *J Biol Chem.* 2002;277:15354-15362.
5. Selbi W, Day AJ, Rugg MS, Fulop C, de la Motte CA, Bowen T, Hascall VC, Phillips AO. Overexpression of hyaluronan synthase 2 alters hyaluronan distribution and function in proximal tubular epithelial cells. *J Am Soc Nephrol.* 2006;17:1553-1567.
6. Lee TH, Wisniewski HG, Vilcek J. A novel secretory tumor necrosis factor-inducible protein (TSG-6) is a member of the family of hyaluronate binding proteins, closely related to the adhesion receptor CD44. *J Cell Biol.* 1992;116:545-557.

7. Day AJ, Aplin RT, Willis AC. Overexpression, purification, and refolding of link module from human TSG-6 in Escherichia coli: effect of temperature, media, and mutagenesis on lysine misincorporation at arginine AGA codons. *Protein Expr Purif.* 1996;8:1-16.
8. Kahmann JD, Koruth R, Day AJ. Method for quantitative refolding of the link module from human TSG-6. *Protein Expr Purif.* 1997;9:315-318.
9. Kuznetsova SA, Mahoney DJ, Martin-Manso G, Ali T, Nentwich HA, Sipes JM, Zeng B, Vogel T, Day AJ, Roberts DD. TSG-6 binds via its CUB_C domain to the cell-binding domain of fibronectin and increases fibronectin matrix assembly. *Matrix Biol.* 2008;27:201-210.
10. Fujimoto T, Savani RC, Watari M, Day AJ, Strauss JF, 3rd. Induction of the hyaluronic acid-binding protein, tumor necrosis factor-stimulated gene-6, in cervical smooth muscle cells by tumor necrosis factor-alpha and prostaglandin E(2). *Am J Pathol.* 2002;160:1495-1502.
11. Lesley J, English NM, Gal I, Mikecz K, Day AJ, Hyman R. Hyaluronan binding properties of a CD44 chimera containing the link module of TSG-6. *J Biol Chem.* 2002;277:26600-26608.
12. Rusnati M, Camozzi M, Moroni E, Bottazzi B, Peri G, Indraccolo S, Amadori A, Mantovani A, Presta M. Selective recognition of fibroblast growth factor-2 by the long pentraxin PTX3 inhibits angiogenesis. *Blood.* 2004;104:92-99.
13. Esko JD. Genetic analysis of proteoglycan structure, function and metabolism. *Curr Opin Cell Biol.* 1991;3:805-816.
14. Liekens S, Leali D, Neyts J, Esnouf R, Rusnati M, Dell'Era P, Maudgal PC, De Clercq E, Presta M. Modulation of fibroblast growth factor-2 receptor binding, signaling, and mitogenic activity by heparin-mimicking polysulfonated compounds. *Mol Pharmacol.* 1999;56:204-213.
15. Camozzi M, Rusnati M, Bugatti A, Bottazzi B, Mantovani A, Bastone A, Inforzato A, Vincenti S, Bracci L, Mastroianni D, Presta M. Identification of an antiangiogenic FGF2-binding site in the N terminus of the soluble pattern recognition receptor PTX3. *J Biol Chem.* 2006;281:22605-22613.
16. Leali D, Belleri M, Urbinati C, Coltrini D, Oreste P, Zoppetti G, Ribatti D, Rusnati M, Presta M. Fibroblast growth factor-2 antagonist activity and angiostatic capacity of sulfated Escherichia coli K5 polysaccharide derivatives. *J Biol Chem.* 2001;276:37900-37908.
17. Ribatti D, Nico B, Vacca A, Presta M. The gelatin sponge-chorioallantoic membrane assay. *Nat Protoc.* 2006;1:85-91.

18. Knoll A, Schmidt S, Chapman M, Wiley D, Bulgrin J, Blank J, Kirchner L. A comparison of two controlled-release delivery systems for the delivery of amiloride to control angiogenesis. *Microvasc Res.* 1999;58:1-9.
19. Garlanda C, Hirsch E, Bozza S, Salustri A, De Acetis M, Nota R, Maccagno A, Riva F, Bottazzi B, Peri G, Doni A, Vago L, Botto M, De Santis R, Carminati P, Siracusa G, Altruda F, Vecchi A, Romani L, Mantovani A. Non-redundant role of the long pentraxin PTX3 in anti-fungal innate immune response *Nature*. England; 2002.
20. Leali D, Alessi P, Coltrini D, Ronca R, Corsini M, Nardo G, Indraccolo S, Presta M. Long pentraxin-3 inhibits FGF8b-dependent angiogenesis and growth of steroid hormone-regulated tumors *Mol Cancer Ther*. United States; 2011.
21. Inforzato A, Baldock C, Jowitt TA, Holmes DF, Lindstedt R, Marcellini M, Rivieccio V, Briggs DC, Kadler KE, Verdoliva A, Bottazzi B, Mantovani A, Salvatori G, Day AJ. The angiogenic inhibitor long pentraxin PTX3 forms an asymmetric octamer with two binding sites for FGF2. *J Biol Chem.* 2010;285:17681-17692.

Supplemental Figure Legends

Supplemental Figure I. Determination of the affinity for the interaction of TSG-6 with PTX3. **A**) Wild-type TSG-6 and TSG-6 mutants with reduced HA-binding capacity (TSG-6_{Y94F}), IαI-heavy chain transfer activity (TSG-6_{E183S}), or both (TSG-6_{Y47F}) were injected onto a PTX3-coated sensorchip and protein binding was monitored by surface plasmon resonance (BIAcore). Sensorgrams (i.e. plots of resonance *vs* time) are reported that are representative of the binding response at analyte concentration of 100 nmol/L for TSG-6_{Y47F} and of 150 nmol/L for all the other analytes. **B**) Kinetics and affinity determinations on the interactions between PTX3 and TSG-6. The analytes were injected over the PTX3 surface at concentrations ranging from 10 to 500 nmol/L and kinetic association and dissociation constants (k_{on} and k_{off}, respectively) were obtained by fitting the raw sensorgrams with the 1:1 Langmuir binding model using the Biaevaluation software (BIAcore). k_d values were derived from the kinetic parameters ($k_d = k_{off}/k_{on}$).

Supplemental Figure II. TSG-6 inhibits the binding of PTX3 to FGF2 in solution. FGF2 (11 pmoles) was incubated with PTX3 (55 pmoles) and the cross-linking reagent BS^3 in the absence or presence of TSG-6 (110 pmoles). The cross-linked proteins were separated on SDS-PAGE gels and detected by Western blotting using either anti-FGF2 or anti-PTX3 antibodies. PTX3 alone and TSG-6 solutions containing either FGF2 or PTX3 were reacted with BS^3 and run as controls. The formation of the PTX3/FGF2 complex with an apparent molecular mass of approx. 180-190 (arrow), in keeping with a PTX3 tetramer/FGF2 monomer complex [21], is inhibited by TSG-6.

Supplemental Figure III. TSG-6 restores HSPG/FGF2/FGFR ternary complex formation inhibited by N_{term}PTX3. A745 CHO flg-1A cells overexpressing FGFR1 were incubated on a monolayer of CHO-K1 cells with mixtures of FGF2 (1.66 nmol/L), N_{term}PTX3 (220 nmol/L) and TSG-6 (56 nmol/L). Bound cells were counted under an inverted microscope after 2 hours of incubation. Data are expressed as percentage of the cell-cell adhesion induced by FGF2 alone (mean of 8 determinations ± SD). Binding of vehicle (PBS)-treated cells (i.e. in the absence of all proteins) is shown as a negative control.

Supplemental Figure IV. TSG-6 mutants rescue FGF2-dependent EC proliferation inhibited by exogenous (**A**) or endogenous (**B**) PTX3. **A**) GM7373 cells were incubated with 0.4% FCS containing 0.56 nmol/L FGF2, 220 nmol/L PTX3 and increasing concentrations of wild-type TSG-6 or TSG-6 mutants with reduced HA-binding capacity (TSG-6_{Y94F}), IαI-heavy chain transfer activity

(TSG-6_{E183S}), or both (TSG-6_{Y47F}). After 24 hours cells were trypsinized and counted. Data are expressed as percentage of GM7373 cell proliferation stimulated by FGF2 only. **B**) Retrovirus-infected MAECs overexpressing human PTX3 (PTX3_MAECs) were incubated with 0.4% FCS *plus* 0.56 nmol/L FGF2 and the indicated amounts of wildtype or mutant TSG-6. Following 24 hours of incubation, cells were trypsinized and counted. Data are expressed as percent of the proliferation measured in mock_MAECs treated with FGF2 alone. Data are the mean ± SD of three experiments performed in triplicate.

Supplemental Figure V. PTX3, FGF2, TSG-6 and VEGF-A expression in murine sub cutaneous Matrigel plugs. Wild-type and *Ptx3*-null female mice were injected s.c. with 400 μL of Matrigel. After 7 days, pellets were processed for total RNA extraction and the levels of PTX3, FGF2, TSG-6 and VEGF-A transcripts were evaluated by semi-quantitative RT-PCR in two representative samples.

Supplemental Figure VI. PTX3, FGF2 and TSG-6 expression and distribution in different human pathological conditions. PPA: pleomorphic parotid adenoma (panels a, b and c); HGM: overlying hyperplastic mucosa in gastric carcinoma (panels d, e and f); AP: atherosclerotic plaque (panels g, h and i). Consecutive tissue sections were immunostained for PTX3, FGF2 and TSG-6, as reported in Methods (brown staining). For each pathological condition, similar results were obtained in specimens from 2-3 patients.
PPA and HGM: a strong and diffuse extracellular PTX3 immunostaining is found in the fibromyxoid stroma of pleomorphic parotid adenoma (**, panel a) and in the superficial lamina propria of hyperplastic gastric mucosa overlying gastric carcinoma (**, panel d); FGF2 and TSG-6 show a prevalent cellular localization, in the cytoplasm of adenoma glands (*, panels b and c respectively) or hyperplastic gastric glands (*, panels e and f respectively).
AP: PTX3 is observed in the core of atherosclerotic plaque, with an extracellular pattern of distribution (**, panel g); FGF2 and TSG-6 are expressed in the cytoplasm of foamy macrophages (arrows indicate representative cells, panels h and i), FGF2 being more intense and diffuse than TSG-6.
(Immunohistochemistry, DAB, Haematoxylin counterstaining, OM 20x).

Supplemental Figure I

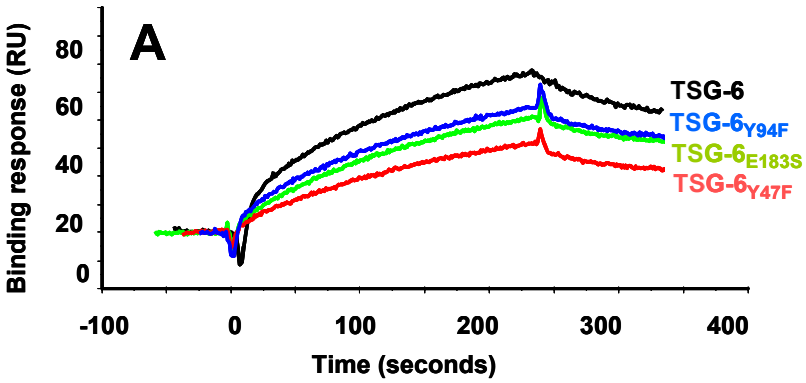

B

Soluble analyte	k_{on} (mol^{-1}/L^{-1} x $seconds^{-1}$)	k_{off} ($seconds^{-1}$)	k_d (nmol/L)
TSG-6	3.01×10^{4}	9.48×10^{-3}	314
Link_TSG6	2.72×10^{4}	17.7×10^{-3}	648
$TSG\text{-}6_{Y47F}$	5.80×10^{3}	11.2×10^{-3}	1,940
$TSG\text{-}6_{Y94F}$	3.31×10^{4}	6.33×10^{-3}	191
$TSG\text{-}6_{E183S}$	2.54×10^{4}	10.5×10^{-3}	415

Supplemental Figure II

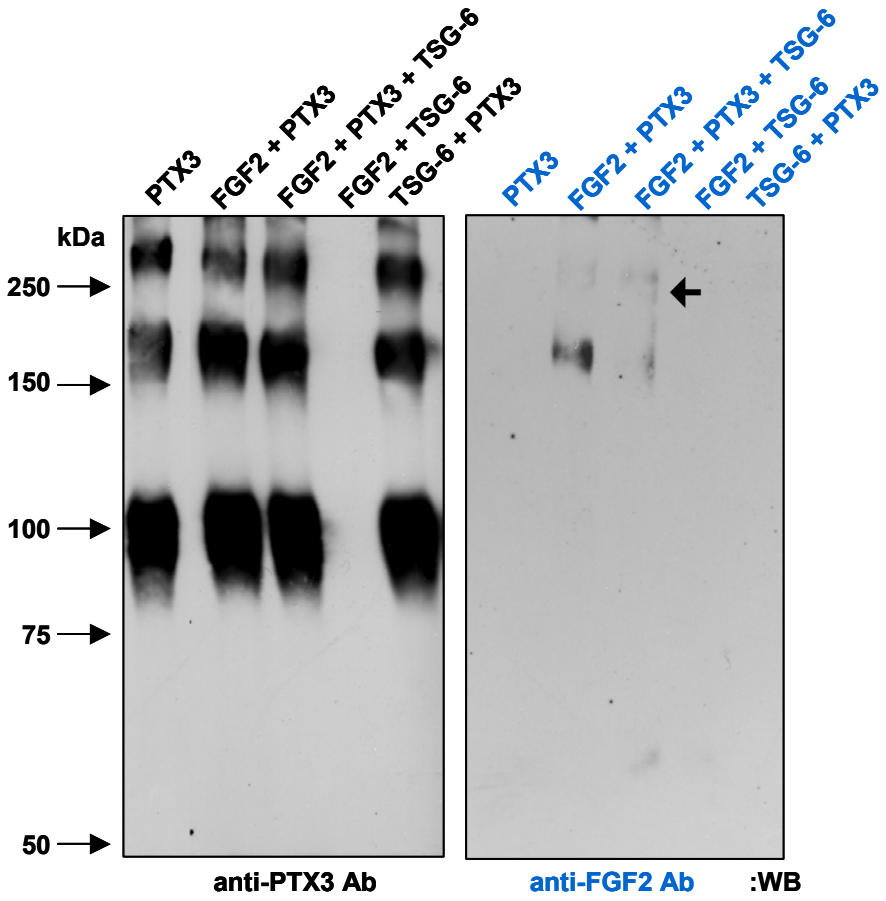

Supplemental Figure III

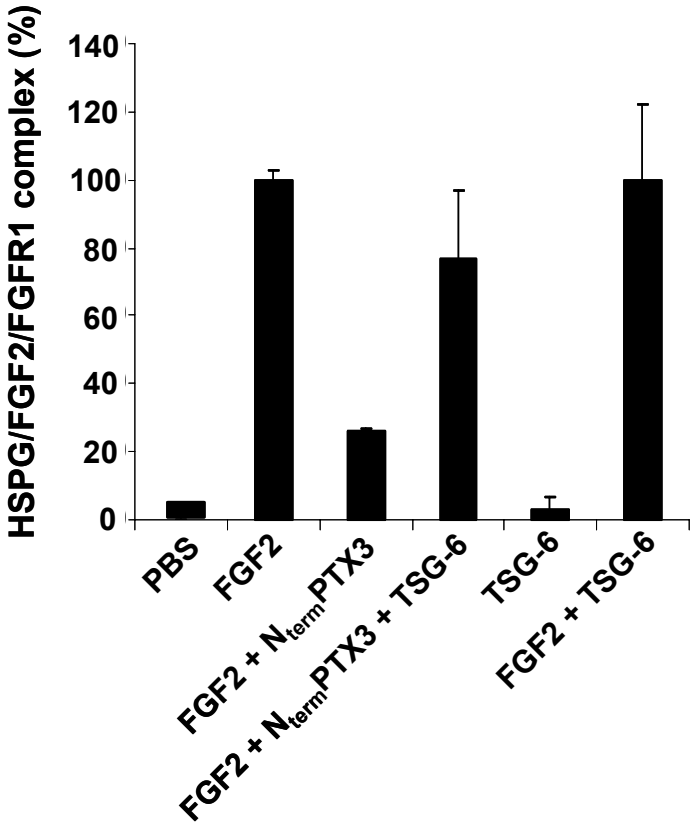

Supplemental Figure IV

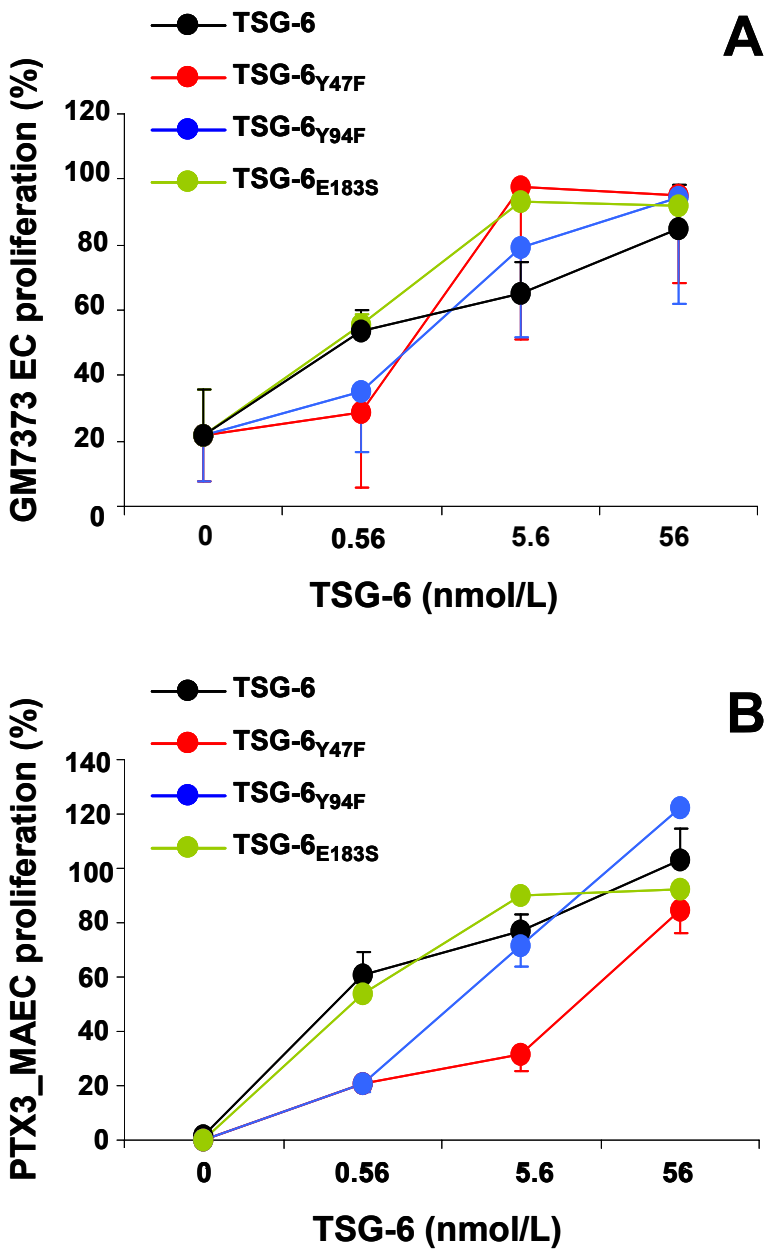

Supplemental Figure V

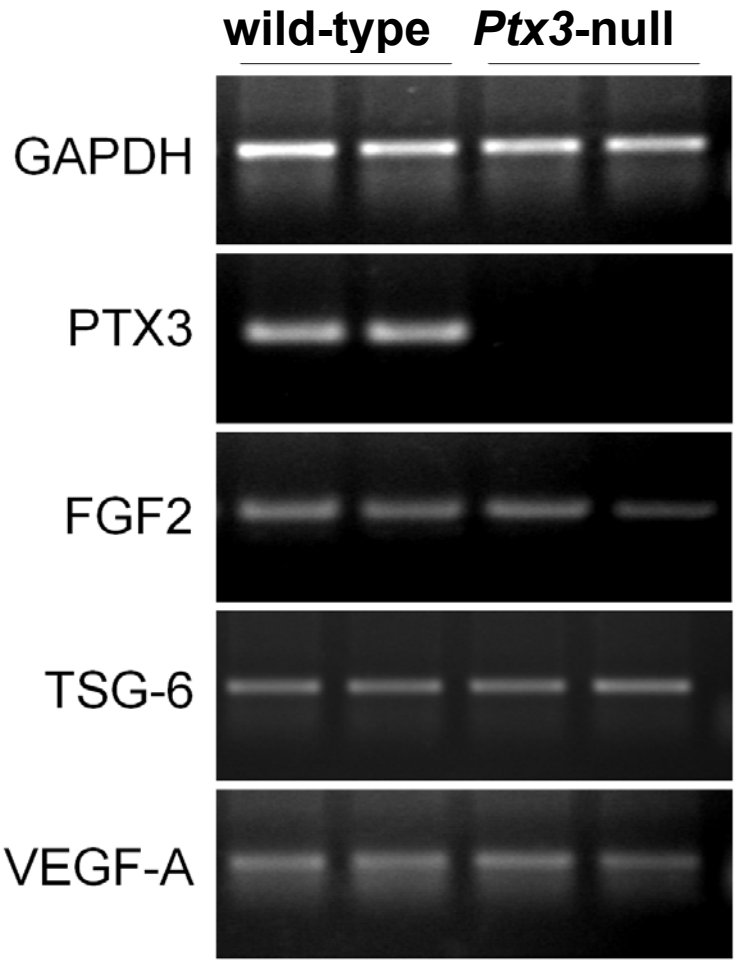

Supplemental Figure VI